# Magnetic Field Saturation in the Riga Dynamo Experiment

Agris Gailitis, Olgerts Lielausis, Ernests Platacis, Sergej Dement'ev, and Arnis Cifersons
*Institute of Physics, Latvian University, LV-2169 Salaspils 1, Riga, Latvia*

Gunter Gerbeth, Thomas Gundrum, and Frank Stefani
*Forschungszentrum Rossendorf, P.O. Box 510119, D-01314 Dresden, Germany*

Michael Christen and Gotthard Will
*Department of Mechanical Engineering, Dresden University of Technology, P.O. Box 01062, Dresden, Germany*
(Received 18 October 2000)

After the dynamo experiment in November 1999 [A. Gailitis *et al.,* Phys. Rev. Lett. **84**, 4365 (2000)] had shown magnetic field self-excitation in a spiraling liquid metal flow, in a second series of experiments emphasis was placed on the magnetic field saturation regime as the next principal step in the dynamo process. The dependence of the strength of the magnetic field on the rotation rate is studied. Various features of the saturated magnetic field are outlined and possible saturation mechanisms are discussed.

DOI: 10.1103/PhysRevLett.86.3024 PACS numbers: 47.65.+a, 52.65.Kj, 91.25.Cw

In the last few decades, the theory of homogeneous dynamos has been unrivaled in explaining magnetic fields of planets, stars, and galaxies. Enormous progress has been made in the numerical treatment of the so-called kinematic dynamo problem where the velocity $\mathbf{v}$ of the fluid with electrical conductivity $\sigma$ is assumed to be given and the behavior of the magnetic field $\mathbf{B}$ is governed by the induction equation

$$\frac{\partial \mathbf{B}}{\partial t} = \nabla \times (\mathbf{v} \times \mathbf{B}) + \frac{1}{\mu_0 \sigma} \Delta \mathbf{B}. \qquad (1)$$

Above a critical value of the magnetic Reynolds number $Rm = \mu_0 \sigma L v$, where $L$ and $v$ denote a typical length and velocity scale of the fluid, respectively, the obvious solution $\mathbf{B} = 0$ of Eq. (1) may become unstable and self-excitation of a magnetic field may occur. The investigation of the saturation mechanism which limits the exponential growth of the magnetic field is much more involved as it requires the simultaneous solution of Eq. (1) and the Navier-Stokes equation

$$\frac{\partial \mathbf{v}}{\partial t} + (\mathbf{v} \cdot \nabla)\mathbf{v} = -\frac{\nabla p}{\rho} + \frac{1}{\mu_0 \rho} (\nabla \times \mathbf{B}) \times \mathbf{B} + \nu \Delta \mathbf{v}, \qquad (2)$$

where the back-reaction of the magnetic field on the velocity is included. In Eq. (2), $\rho$ and $\nu$ denote the density and the kinematic viscosity of the fluid, respectively.

A number of recent computer simulations of the Earth's core have led to impressive similarities between the computed and the observed magnetic field behavior including, most remarkably, field reversals [1]. The actual relevance of these simulations for real dynamos is, however, not completely clear as they are either working in parameter regions far from that of the Earth or have to resort to numerical trickery as, e.g., the use of anisotropic hyperdiffusivities (for a recent overview, see [2]).

Until very recently, a serious problem of the science of hydromagnetic dynamos was the lack of any possibility to verify numerical results by experimental work. This situation changed on 11 November 1999 when in the first Riga dynamo experiment self-excitation of a slowly growing magnetic field eigenmode was observed for the first time in an experimental liquid metal facility [3]. On the background of an amplified external signal, the growth rate and the rotation frequency of the self-excited field were identified to be in good agreement with the numerical predictions based on kinematic dynamo theory. Because of some technical problems, the saturation regime was not reached in this first experiment. Soon after, Müller and Stieglitz studied self-excitation and the saturation regime in another dynamo facility in Karlsruhe [4].

In the following we represent the results of a second series of experiments at the Riga facility which were carried out during 22–25 July 2000. It was possible to work at considerably lower sodium temperatures and thus at higher electrical conductivities than in the November experiment. This fact allowed us to study in great detail the dynamo behavior in the kinematic as well as in the saturation regime. Here, we mainly focus on the results in the saturation regime as they go essentially beyond the results of the November 1999 experiment.

The Riga dynamo facility consists of three concentric tubes of approximately 3 m length (Fig. 1). In the innermost tube of 25 cm diameter a spiraling flow of liquid sodium with a velocity up to 15 m/s is produced by a propeller. The sodium flows straight back in a second coaxial tube and stays at rest in a third outermost tube. For more details of the experimental design, see [3] and references therein.

As in November 1999, the $r$ component of the magnetic field outside the dynamo was measured by Hall sensors at eight different places, six of which were aligned parallel to the axis. Within the dynamo, close to the

 0031-9007/01/86(14)/3024(4)$15.00 

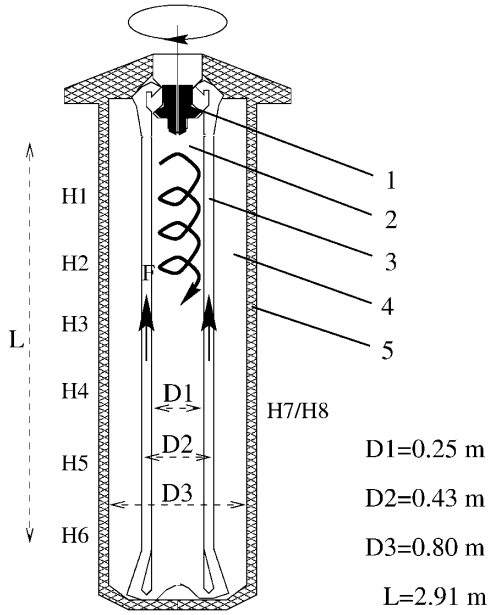


FIG. 1. The main part of the Riga dynamo facility: 1—Propeller; 2—Helical flow region; 3—back-flow region; 4—sodium at rest; 5—thermal insulation; F—position of the flux-gate sensor and the induction coil; H1, . . . , H6—positions of six aligned Hall sensors; H7/H8—two Hall sensors at different azimuths.

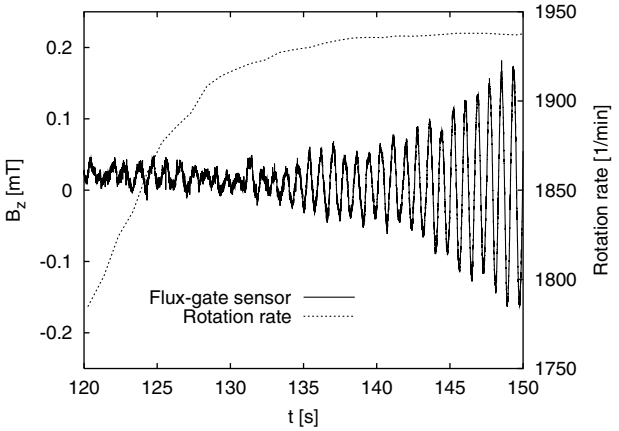


FIG. 2. The signal from the inner flux-gate sensor (F in Fig. 1) at the beginning of magnetic field self-excitation together with the rotation rate. The temperature was 170.5°C.

innermost wall, the $z$ component of the magnetic field was measured by a sensitive flux-gate magnetometer to study the starting phase of field generation and the $r$ component by a less sensitive induction coil recording over all the generation time.

A typical run is documented in Figs. 2 and 3. Without any external excitation, a rotating field starts to grow exponentially around $t = 130$ s when the rotation rate has reached 1920 $\text{min}^{-1}$ (Fig. 2). Starting with this moment the rotation rate was kept practically constant for 80 s (Figs. 3a and 3b). The whole magnetic field pattern rotates around the vertical axis in the direction of the propeller rotation, but much slower. Hence, each sensor records an ac signal with a frequency of the order 1 Hz.

After increasing the rotation rate to about 2020 $\text{min}^{-1}$ at $t \approx 220$ s the exponential growth becomes faster. At $t \approx 240$ s the exponential growth goes over into saturation where the magnetic field continues to rotate with a certain frequency but stays essentially constant in its amplitude (Fig. 3c). Between $t \approx 240$ s and $t \approx 350$ s different rotation rates have been studied, showing a clear dependence of the saturation field level on the rotation rate. For a period of 10 s, Fig. 3c shows in detail the induction coil signal recorded at regular 0.04 s time intervals. Putting attention on the placement of points, some turbulence caused deviation from the main sinusoidal signal is clearly seen. The detailed analysis of the turbulence is left for further work.

From a total of four experimental runs similar to that shown in Fig. 3, together with the November experiment, we compiled a number of data concerning the rotation rate dependence of the growth rates (Fig. 4a), of the frequencies (Fig. 4b), of the power consumption of the motors (Fig. 5), and of the saturation levels (Fig. 6).

Figure 4 shows the numerical prediction and the measured data for the growth rate (a) and the frequency (b). The numerical prediction is based on a time-dependent 2D finite difference solver for the kinematic dynamo problem in the real finite cylinder geometry using the velocity profiles measured during a water test run at the facility (for details, see [5]). For the sake of clarity, we have chosen one reference temperature for the prediction and we have scaled all measured data to this temperature by taking into account the temperature dependence of the electrical conductivity. As a reference temperature we have chosen $T = 157\,^{\circ}\text{C}$, simply for the reason that this was the temperature where (in one run) at a rotation rate of 1840 $\text{min}^{-1}$ an extremely slowly decaying mode was observed which is considered as a reference state. Therefore, the propeller rotation rate $\Omega$ as well as the growth rate $p$ and the frequency $f$ at the temperature $T$ were scaled to $(\Omega_c, p_c, f_c) = \sigma(T)/\sigma(157\,^{\circ}\text{C})\,[\Omega(T), p(T), f(T)]$ as required by the scaling properties of Eq. (1). By virtue of this definition, the corrected rotation rate $\Omega_c$ is proportional to the magnetic Reynolds number $Rm$.

The data in Fig. 4 show a satisfactory correspondence with the numerical prediction, in particular, concerning the slope of the curves. In both cases, the difference between the data and the prediction consists in a horizontal shift of a few percent. The shift of the growth rates is partly caused by the fact that the internal steel walls (with their lower electrical conductivity) were not taken into account in the 2D code underlying the given numerical predictions [5]. One-dimensional calculations had revealed [6] that these walls give rise to an increase of the critical $Rm$ by about

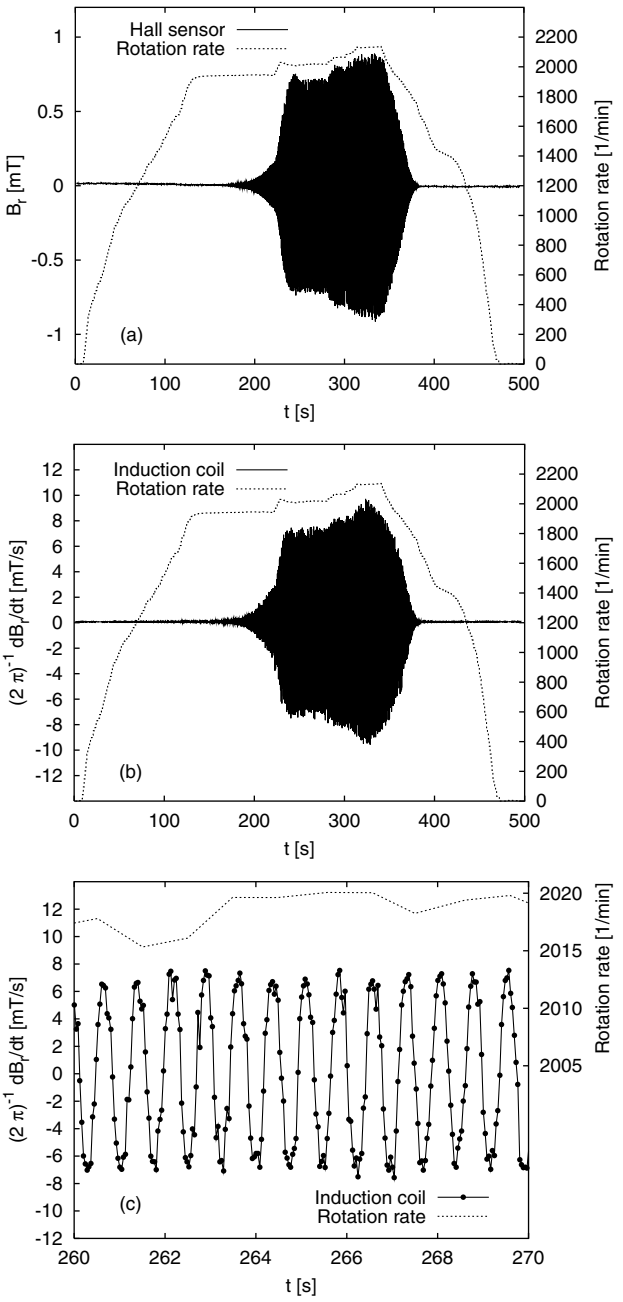


FIG. 3. One of the experimental runs with self-excitation and saturation: signals measured at the Hall sensor H4 (a) and in the induction coil at position F (b). A zoomed fragment of (b) is shown in (c).

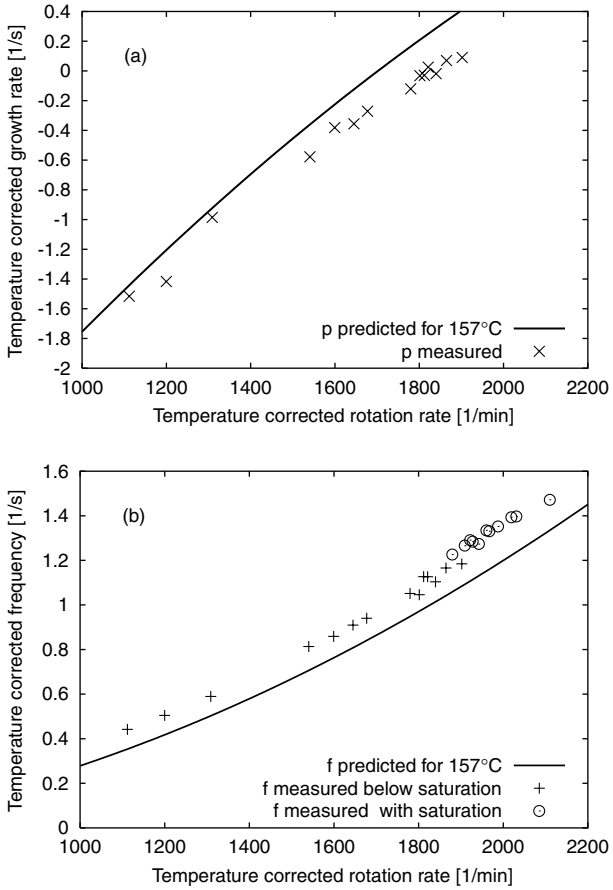


FIG. 4. Growth rates (a) and frequencies (b) for different rotation rates and temperatures in comparison with the numerical prediction. In (b) the frequencies in the saturation regime are also given, whereas the corresponding growth rates are zero.

8% which agrees with the said parallel shift. In total, there is now quite a coherent picture of the kinematic regime in which the results from the November experiment and the recent results fit together.

As for the saturation regime, there is an interesting observation to be made in Fig. 4b. Whereas in this regime the growth rates are zero, the frequencies continue to increase with the rotation rate (the frequency values seem even a bit higher than what would be expected from a simple extrapolation of the data in the kinematic regime). This fact indicates that there is not only an overall break of the sodium flow by the Lorentz forces but that the spatial structure of the flow is changed, too.

Concerning the motor power increase in the saturation regime we show in Fig. 5 for one experimental run the motor power consumption as a function of the rotation rate $\Omega$. The points in Fig. 5 correspond to those time intervals where the rotation rate was kept constant. The shown data in the field-free regime are best fitted with an $\Omega^3$ curve which is also expected from simple hydraulic arguments. As for the four rightmost points in the saturation regime, there is evidently an increase of the power consumption which must be explained in terms of the back-reaction of the magnetic field. In order to estimate this additional power the Ohmic losses $P_{\mathrm{Ohm}} = \int j^2/\sigma \, dV$ have to be computed. Using the magnetic field structure as it results from the kinematic code and fixing its strength to the measured field strength we get Ohmic losses of approximately 10 kW which agrees with the observed power consumption increase.

However, as already mentioned in connection with the observed frequency behavior, the power increase due to magnetic forces is not the whole story. Another feature of

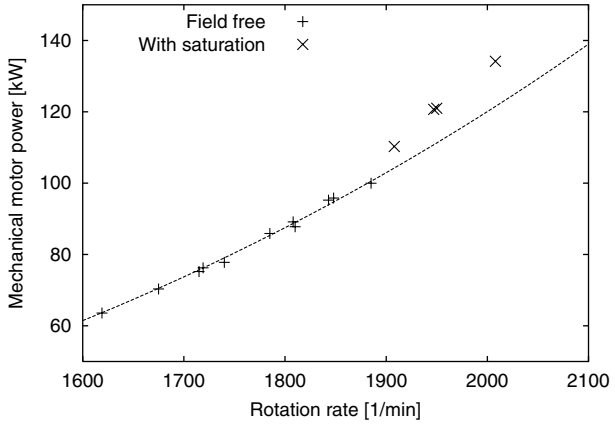


FIG. 5. Motor power below and in the saturation regime.

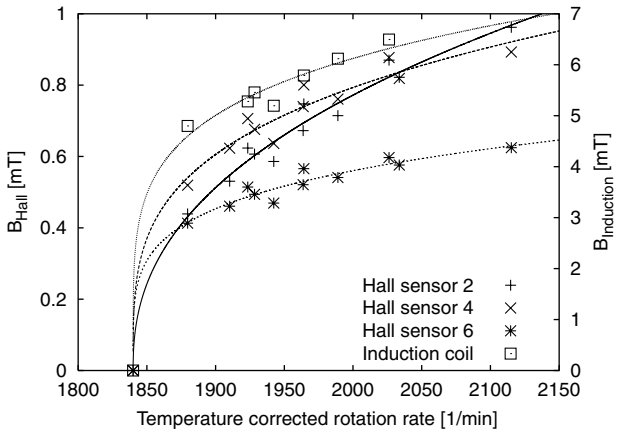


FIG. 6. Measured magnetic field levels in the saturation regime. The lines are fitting curves of the form $\sim(\Omega_c - 1840\ \mathrm{min}^{-1})^{\beta}$ with $\beta = 0.417$ for H2, $\beta = 0.275$ for H4, $\beta = 0.216$ for H6, and $\beta = 0.205$ for the induction coil.

the field might help to identify a further saturation mechanism. In Fig. 6 we have plotted four saturation levels of the radial magnetic field component measured at different positions in dependence on the temperature corrected rotation rate $\Omega_c$. Three of the measurements were carried out at the Hall sensors H2, H4, H6 (see Fig. 1). The fourth field is inferred from the induced voltage (divided by the frequency) in the induction coil at position F. The magnitude of the radial component reaches 7 mT. From numerical simulations of the kinematic regime it is known that the axial component at the given position is by a factor of 5 larger than the radial component. Hence a value of about 35 mT seems to be a reasonable estimate for this $z$ component inside the dynamo. The four different saturation levels in Fig. 6 are fitted by some curves proportional to $(\Omega_c - 1840\ \mathrm{min}^{-1})^{\beta}$ (the behavior close to $\Omega = 1840\ \mathrm{min}^{-1}$ might be different, however, as a slightly subcritical part close to the marginal point cannot be excluded by our data). The different exponents give clear evidence for a remarkable redistribution of the magnetic energy towards the propeller region.

This phenomenon, together with the above mentioned fact that the frequency continues to grow in the saturation regime, could be explained by an axial variation of the velocity profile under the back-reaction of the magnetic field. The decisive effect comes from the downward accumulating reduction of the azimuthal velocity due to the azimuthal component of the Lorentz force, whereas the axial component of the Lorentz force will mainly be absorbed into a pressure gradient resulting in the discussed motor power increase.

In [7] we have studied the effect of axially varying velocity profiles by means of the 2D kinematic code. For a given velocity at the propeller, a stronger downward decay of the azimuthal velocity resulted in a significant decrease of the growth rate, in a nearly unchanged frequency, and in an upward shift of the magnetic field pattern. Therefore, this downward decay is a favorite candidate to account for the observed features of the magnetic field in the saturation regime.

The study of the saturation regime will be continued by means of numerical simulations in tight connection with a sort of inverse dynamo approach based on the measured data and, hopefully, with direct velocity measurements inside the dynamo facility.

We thank the Latvian Science Council for support under Grant No. 96.0276, the Latvian Government and International Science Foundation for support under joint Grant No. LJD100, the International Science Foundation for support under Grant No. LFD000, and Deutsche Forschungsgemeinschaft for support under INK 18/B1-1.

[1] G. A. Glatzmaier and P. H. Roberts, Nature (London) **377**, 203 (1995).
[2] F. H. Busse, Annu. Rev. Fluid Mech. **31**, 383 (2000).
[3] A. Gailitis *et al.,* Phys. Rev. Lett. **84**, 4365 (2000).
[4] U. Müller and R. Stieglitz, Naturwissenschaften **87**, 381 (2000).
[5] F. Stefani, G. Gerbeth, and A. Gailitis, in *Transfer Phenomena in Magnetohydrodynamic and Electroconducting Flows,* edited by A. Alemany, Ph. Marty, and J. P. Thibault (Kluwer Academic Publishers, Dordrecht, The Netherlands, 1999), p. 31.
[6] A. Gailitis, Magnetohydrodynamics **32**, 58 (1996).
[7] F. Stefani, G. Gerbeth, and A. Gailitis, in *Proceedings of the International Workshop on Laboratory Experiments on Dynamo Action, Riga, 1998,* edited by O. Lielausis, A. Gailitis, G. Gerbeth, and F. Stefani, (FZ Rossendorf, Dresden, 1998).